Controlled potential electro-oxidation of genomic DNA

Vytas Reipa*, Donald H. Atha, Sanem H. Coskun, Christopher M. Sims, Bryant C. Nelson

Materials Measurement Laboratory, Biosystems and Biomaterials Division, National Institute of Standards and Technology, Gaithersburg, Maryland, United States of America

* vytas@nist.gov

Abstract

Exposure of mammalian cells to oxidative stress can result in DNA damage that adversely affects many cell processes. Lack of dependable DNA damage reference materials and standardized measurement methods, despite many case-control studies hampers the wider recognition of the link between oxidatively degraded DNA and disease risk. We used bulk electrolysis in an electrochemical system and gas chromatographic mass spectrometric analysis (GC/MS/MS) to control and measure, respectively, the effect of electrochemically produced reactive oxygen species on calf thymus DNA (ct-DNA). DNA was electro-oxidized for 1 h at four fixed oxidizing potentials (E = 0.5 V, 1.0 V, 1.5 V and 2 V (vs Ag/AgCl)) using a high surface area boron-doped diamond (BDD) working electrode (WE) and the resulting DNA damage in the form of oxidatively-modified DNA lesions was measured using GC/MS/MS. We have shown that there are two distinct base lesion formation modes in the explored electrode potential range, corresponding to 0.5 V < E < 1.5 V and E > 1.5 V. Amounts of all four purine lesions were close to a negative control levels up to E = 1.5 V with evidence suggesting higher levels at the lowest potential of this range (E = 0.5 V). A rapid increase in all base lesion yields was measured when ct-DNA was exposed at E = 2 V, the potential at which hydroxyl radicals were efficiently produced by the BDD electrode. The present results demonstrate that controlled potential preparative electrooxidation of double-stranded DNA can be used to purposely increase the levels of oxidatively modified DNA lesions in discrete samples. It is envisioned that these DNA samples may potentially serve as analytical control or quality assurance reference materials for the determination of oxidatively induced DNA damage.

Introduction

Exogenous disturbances (exposure to ionizing radiation or chemical toxicants) or endogenous perturbations (inflammation or elevated iron content) in the normal redox status of cells can produce oxidizing species that can potentially damage cellular components (e.g., proteins, lipids, and DNA) [1]. These oxidizing species, generally known as reactive oxygen species (ROS) can alter the structure of DNA, as well as lead to the formation of oxidatively modified purine and pyrimidine bases, DNA strand breaks, DNA-protein cross-links, abasic sites and

other types of DNA lesions [2]. The reliable measurement of oxidatively induced DNA damage *in vitro* and *in vivo* is critical to the establishment of reference ranges for biomarkers of redox imbalance in health and disease. As was recognized early-on, the overall variation in DNA lesion levels, obtained by different analytical methods may reach up to tenfold even using the same samples derived from human cells [3]. Interlaboratory comparison studies with calf thymus DNA (ct-DNA) samples containing increasing amounts of 8-hydroxyguanine (8-OH-Gua) lesions concluded that control or reference samples with 8-OH-Gua lesion levels close to those found in nature ($\approx$ one lesion per 10^6 DNA bases) are needed to ensure robust and reproducible measurements in human studies [4]. 8-OH-Gua is not only an important DNA damage lesion but also a recognized biomarker of oxidative stress. Lack of dependable DNA damage reference materials and standardized measurement methods, despite many case-control studies, hampers the wider recognition of the link between oxidatively damaged DNA and disease.

The effective redox potential is a specific metric that can be used to quantify the relative strength of different oxidizing agents, including different types of ROS. Hydroxyl radicals ($^\bullet$OH), although short-lived ($\tau \approx 10^{-9}$s) [5], are one of the strongest oxidants generated in aqueous environments with a formal potential of $E_7 = +1.9$ V (Ag/AgCl, saturated KCl) [6]. Other ROS such as hydrogen peroxide (H_2O_2): $E_7 = +0.6$ V [6] or superoxide radical ($O_2^{\bullet-}$): $E_7 = -0.13$ V [7] are less potent, but more stable in solution. Establishing the relationship between the strength/power of the exogenous oxidative action, characterized by the imposed redox potential, and the subsequent biomolecular consequences is essential for characterizing the mechanistic framework of oxidative damage [8]. Environments that induce oxidative stress in biological experiments are traditionally generated via exposure to ionizing radiation, UV light or oxygen. Exposure to chemical agents or chemical reactions that produce ROS can also produce oxidizing environments [9]. However, in many of these exposure scenarios the oxidant strength is hard to control and quantify in such environments and is typically presented in relative and/or qualitative terms that impedes data comparison across laboratories.

DNA contains four electroactive bases that can be electrochemically oxidized [10–12]. This important feature led to the development of electrochemical sensors for detecting DNA hybridization and DNA base damage at attomole levels [13]. Electrochemical oxidation is rather slow and irreversible, the rate of which depends on the apparent standard redox potential and a standard rate constant [14]. Numerous electroanalytical studies have determined redox potentials of free bases [15], nucleotides and nucleosides [7, 9] [16–18] and synthetic DNA [19]. At pH 7, free guanine (Gua) is oxidized at +0.7 V (vs Ag/AgCl), adenine (Ade) at +0.97 V, thymine (T) at +1.15 V, and cytosine (Cyt) at +1.31 V [14]. Corresponding redox potentials for nucleotides increase by ≈ 0.25 V for Gua, Ade, Thy and 0.17 V for Cyt [20], while redox potentials for DNA bases inside intact DNA are further modulated by π stacking, hydrogen bonding, chemical modification and shielding of the electroactive moieties [14]. Electrochemical studies on intact single and double-stranded DNA indicate that redox potentials increase in the order of dGua<dAde<dThy<dCyt [21–23] with dThy and dCyt oxidation current waves reportedly overlapping [20]. Electro-oxidation efficiency is highly dependent on DNA structure and percentage of Gua [19]. A compilation of the nucleotide oxidation potentials is presented in Table A in S1 Text.

The oxidation of Gua is an irreversible process that occurs in two steps. The first step requires two protons and two electrons, resulting 8-OH-Gua. Another Gua damage product is 2,6-diamino-4-hydroxy-5-formamidopyrimidine (FapyGua), which forms when the intermediate 8-hydroxy-7,8-dihydroguan-8-yl radical is reduced leading to the opening of the imidazole ring [24]. The Ade oxidation mechanism is similar, resulting in 8-oxo-7,8-dihydroadenine (8-OH-Ade) and 4,6-diamino-5-formamidopyridimidine (FapyAde) as the key stable

products. Ring-opened lesions are cytotoxic as they interfere with DNA synthesis [25]. The Ade oxidation product yield is typically eight- to tenfold lower than the corresponding yields of Gua-derived products [26].

As pyrimidines possess higher oxidation potentials than purines, they would be expected to be less susceptible to oxidative damage based on thermodynamics. Nevertheless, oxidative damage in Ade/Thy rich sequences is observed mostly at Thy due to proton-coupled electron transfer assisted formation of the Thy hydroperoxyl radicals [27]. These radicals may decay via pyrimidine ring cleavage forming 5-hydroxy-5-methylhydantoin derivatives (5-OH-5-MeHyd) [26]. Accumulation of these lesions *in vivo* often indicates potential lethality as it interferes with DNA polymerase function [28].

Most electron transfers in DNA are accompanied by proton transfer, therefore nucleic acid base redox potentials are pH-dependent [29]. When an intact DNA strand is probed with electrochemical techniques, electrical charges can migrate significant distances along the strand [30, 31] facilitating the indirect electro-oxidation of nucleobases [14, 32]. Coupling of preparative electrochemical DNA oxidation with spectroscopic examination of reaction products offers new insights into these processes. Goyal et al. studied the oxidation chemistry of numerous nucleic acid components at various carbon-based electrodes and analyzed the reaction products using ultraviolet-visible (UV-VIS) spectrophotometry, nuclear magnetic resonance (NMR) spectroscopy and mass spectrometry (MS) [16, 33, 34]. Baumann et al. [35] analyzed electrochemical oxidation products of free nucleotides by using an efficient flow-through thin-layer electrochemical cell coupled to real-time product analysis via electrospray ionization mass spectrometry (ESI-MS). Their electrochemical system included a boron doped diamond (BDD) anode that could both abstract electrons directly from DNA in solution as well as produce $^\bullet$OH radicals at high anodic potentials (E $\geq$ 1.8 V).

The goal of the present work was to create a stable and robust solution-state environment for electro-oxidizing genomic DNA samples using controlled potentials in a batch operating mode as a potential pathway to produce DNA damage calibrants. A BDD working electrode (WE) was utilized to establish a stable oxidizing environment, an environment whereby DNA samples with quantifiable levels of oxidatively modified lesions could be produced. Previously, with capillary electrophoresis, we have quantified nucleic acid fragmentation under a constant oxidizing potential treatment using a reticulated carbon WE [36]. Here we equilibrate solution-state DNA with a high surface area BDD WE, biased at constant potentials in the range from 0.5 V to 2.0 V. When polarized at 2V the BDD electrode becomes an efficient $^\bullet$OH radical producer while limiting oxygen evolution due to its high overpotential [37, 38]. The maximum concentration of $^\bullet$OH radicals at the BDD electrode surface may reach several tens of micromoles per liter and the reaction layer can extend up to a micrometer into the electrolyte [39]. Exposure of the continuously agitated DNA solution molecules to a high surface area WE battery enables a steady charge exchange between the DNA and the anodes either directly and through products of solvent electrolysis serving as redox mediators. The reverse reactions at the counter electrode (CE) are suppressed by enclosing the Si CE in dialysis bags (2000 MW cutoff) that prevent direct DNA molecule (average MW of DNA is about 800 000 [40]) access to the CE surface.

Hyphenated mass spectrometry techniques are broadly utilized for the identification and quantification of oxidatively induced DNA damage in cells, tissues and whole organisms. In the present study, ct-DNA in buffered solution was electrochemically-treated (oxidized) using a range of fixed potentials to generate controlled levels of DNA base damage (DNA lesions) within the intact, double-stranded DNA matrix. Following enzymatic release of the DNA lesions from the treated samples, isotope-dilution gas chromatography/tandem mass spectrometry (GC/MS/MS) was utilized to identify and quantify the distribution of generated

DNA lesions at each BDD WE potential. DNA damage profiles generated by direct one electron oxidation at low potentials (E = 0.5 V to 1.5 V) were quantitatively compared against the DNA damage profiles produced by treating the DNA to an oxidative bias at E = 2 V, where $^{\bullet}$OH radicals are known to be efficiently generated.

Materials and methods

Materials

Calf thymus DNA-sodium salt (ct-DNA), potassium phosphate monobasic and potassium phosphate dibasic were purchased from Sigma-Aldrich Corp (St. Louis, MO, USA). 4,6-Diamino-5-formamidopyrimidine-^{13}C,^{15}N$_2$ (Fapy adenine-^{13}C,^{15}N$_2$), 2,6-diamino-4-hydroxy-5-formamidopyrimidine-^{13}C,^{15}N$_2$ (Fapy guanine-^{13}C,^{15}N$_2$), 8-hydroxyadenine-^{15}N$_5$ (8-OH-adenine-^{13}C,^{15}N$_2$), 5-hydroxy-5-methylhydantoin-^{13}C,^{15}N$_2$ (5-OH-5-MeHyd-^{13}C,^{15}N$_2$) and 8-hydroxy-2′-deoxyguanosine-^{15}N$_5$ were purchased from Cambridge Isotope Laboratories (Andover, MA). 8-Hydroxyguanine-^{15}N$_5$ (8-OH-guanine-^{15}N$_5$) was obtained by hydrolysis of 8-hydroxy-2′-deoxyguanosine-^{15}N$_5$ with 60% formic acid at 140˚C for 30 min followed by lyophilizing. Subsequently, 8-OH-guanine-^{15}N$_5$ was dissolved in 10 mmol/L NaOH before use. *E. coli* formamidopyrimdine DNA glycosylase (Fpg) and *E. coli* endonuclease (III) (EndoIII) were purchased from Trevigen (Gaithersburg, MD).

The electrochemical reactor

The stable oxidative environment was created by exposing ct-DNA in solution to the desired WE potential, maintained by an EG&G Model 273 potentiostat (Princeton Applied Research, Inc., Oak Ridge, TN)). Electrochemical cell (see Fig 1) contained a battery of two double-sided BDD WE's (total active area S = 40 cm^2) and three double-sided highly doped Si wafer CE's (S = 60 cm^2) (Virginia Semiconductor, Inc., Fredericksburg, VA), each enclosed in a 2000 MW cutoff dialysis bag (Thermo Fisher Scientific, Waltham, MA). The electrodes were separated by 0.2 mm Teflon gaskets with contact leads produced using silver epoxy. A rectangular 40 mm path-length quartz spectrophotometer cell (Starna Cells, Inc., Atascadero, CA) was used for bulk electrolysis under slow solution mixing by the inert Ar gas purging. A flexible Ag/AgCl electrode (MI-402, Microelectrodes Inc., Bedford, NH) served as a reference electrode (RE). Unless noted otherwise, the potential values throughout this study are quoted relative to the Ag/AgCl, saturated KCl RE (E = 0.199 V vs Normal Hydrogen Electrode). Prior to sample introduction, cell electrodes were activated by potential cycling at 20 mV/s in buffer solution between -1 V and +2.5 V for 30 min.

During potentiostatic treatment, the cell contained 2 mL of DNA solution in 0.01 mol/L potassium phosphate buffer (pH 7.0) at room temperature (20˚C). Following each h exposure at a given WE potential, the DNA solution was removed for analysis, the cell was dismantled, and the electrodes were sonicated for 10 min in a detergent solution (RBS35, Pierce Inc., Rockford, IL), followed by a vigorous rinsing with distilled and deionized (DI) water.

DNA sample preparation and treatment

Calf thymus DNA 0.5 mg/mL was dissolved in DI water using 50 mL Falcon tube. To fully solubilize the stock DNA, the tube was placed on a rocker for 72 h at 4˚C using gentle inversion. Next, the stock solution was dialyzed against DI water using membrane dialysis with a 6 kD cutoff and stored at 4˚C. The DNA concentration was measured by absorbance at 258 nm and was distributed into 50 microgram aliquots. Solutions of DNA at 250 µg/mL in 0.01 mol/L
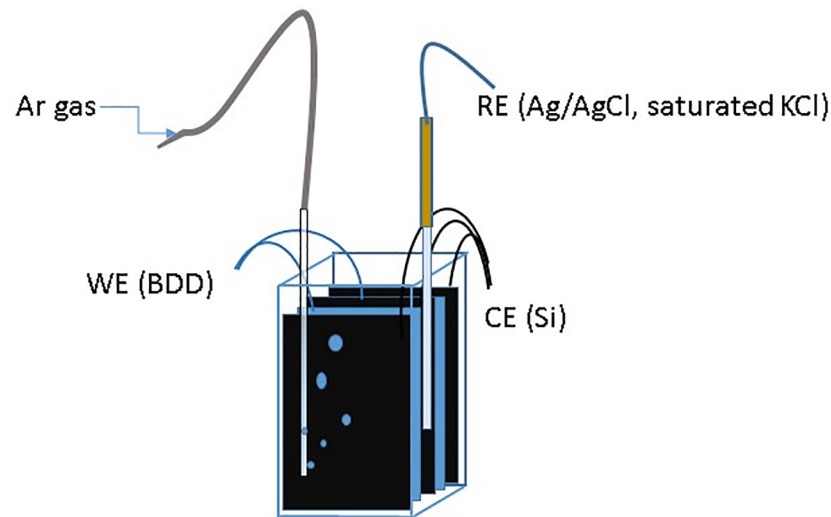
Fig 1. Electrochemical cell used for DNA oxidation. BDD WE is shown in blue, Si CE- black.

potassium phosphate buffer (pH 6.9) were prepared for each electrochemical treatment as well as controls for GC/MS/MS.

Measurement of DNA base lesions by isotope-dilution GC/MS/MS

Samples containing 50 μg of genomic DNA were enzymatically digested and analyzed using isotope-dilution GC/MS/MS based upon procedures described in previous studies [41–46]. The following DNA base lesions were reproducibly detected and quantified in electrochemically oxidized DNA samples: FapyAde and 8-OH-Ade (Ade-derived lesions), 5-OH-5-MeHyd (T-derived lesion) and FapyGua and 8-OH-Gua (Gua-derived lesions) (Fig 2). The reproducible detection and quantification of 5-OH-Cyt (Cyt-derived lesion) was not possible using our currently developed GC/MS/MS procedure due to interference from an overlapping component having the same retention time and mass/charge (m/z) ratio as 5-OH-Cyt. 40 Gy gamma irradiated Ct-DNA was used as a positive control. Full details of the methodology are available in the S1 Text.

Statistical analysis

All statistical analyses were conducted with GraphPad Prism 6.0. Statistical tests and criteria for the reported results are given in the respective Figure legends.

Results

The selected potential range encompassed the known oxidation potentials of the four DNA bases [23, 29, 47]. At the highest applied potential, E = 2 V, the BDD WE is also known to produce significant quantities of ⋅OH radicals through H_2O electrolysis [38].

DNA solutions at 250 μg/mL were loaded into the electrochemical cell, slowly purged with inert gas for 30 min at the open circuit potential and a fixed potential was applied to the WE for 1 h with values: 0.5 V, 1.0 V, 1.5 V and 2.0 V. As evident from the current-time trace, recorded during 2 V potentiostatic treatment (Fig 3, upper panel), the solution species establish a redox equilibrium with WE in about 20 min. following potential application, while at lower applied potentials the cell current was very low, indicating an exhaustive DNA
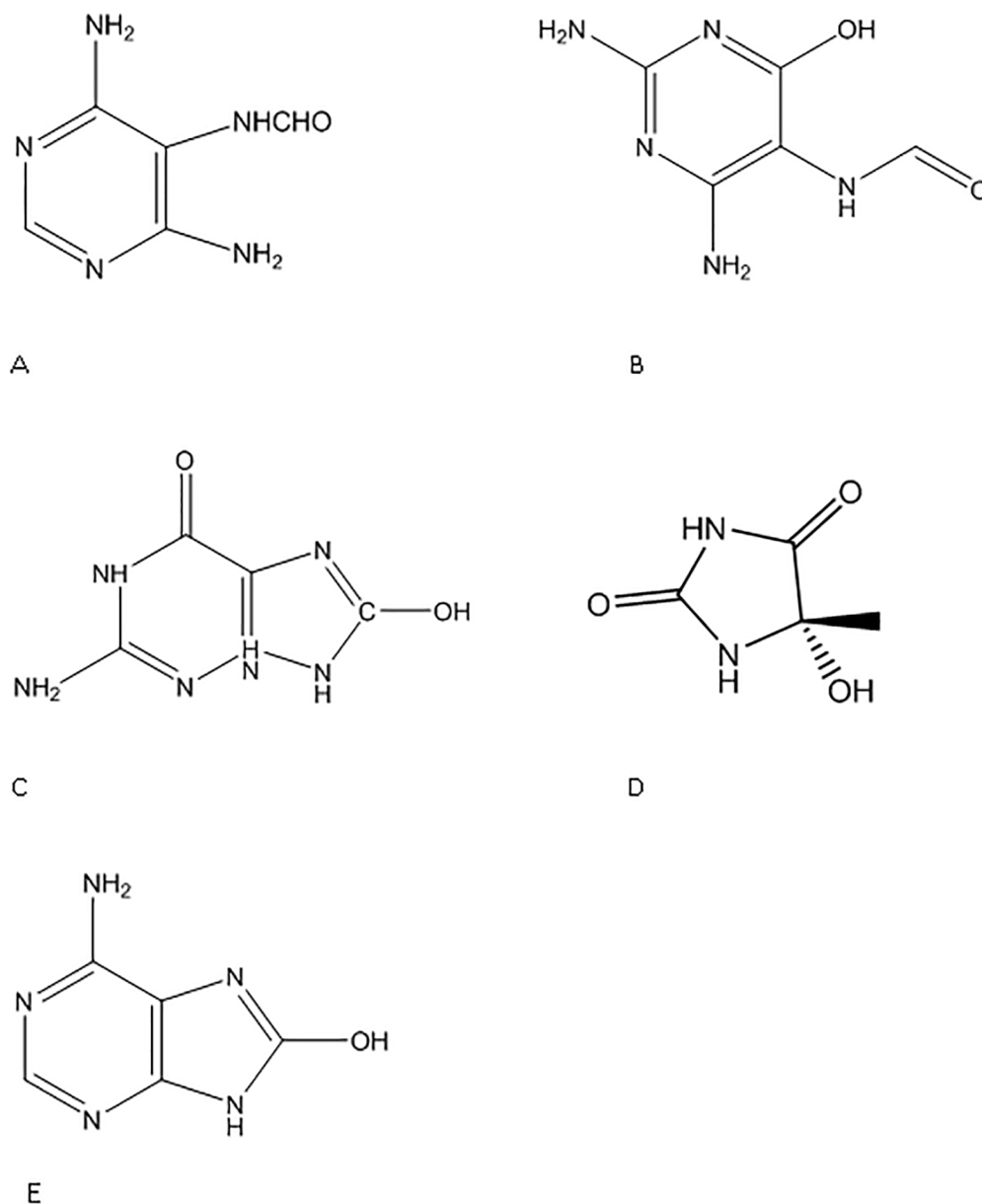
Fig 2. Oxidatively modified DNA base lesions measured in this study. (A) 4,6 diamino-5-formamidopyrimidine (FapyAde), (B) 2,6-diamino-4 hydroxy-5-formamidopyrimidine (FapyGua), (C) 8-hydroxyguanine (8-OH-Gua), (D) 5-hydroxy-5-methylhydantoin (5-OH-5-MeHyd), and (E) 8 -hydroxyadenine (8-OH-Ade).

https://doi.org/10.1371/journal.pone.0190907.g002

electrolysis. A slow linear current-potential scan, recorded in the same solution (Fig 3, lower panel) shows that the cell current starts increasing at E > 1.6 V due to the start of the H_2O oxidation reactions at the BDD WE. As shown previously [48, 49], H_2O oxidation on BDD electrodes proceeds via efficient generation of the $^\bullet OH$ radicals:

$$H_2O \rightarrow \cdot OH + H^+ + e^-, \tag{1}$$
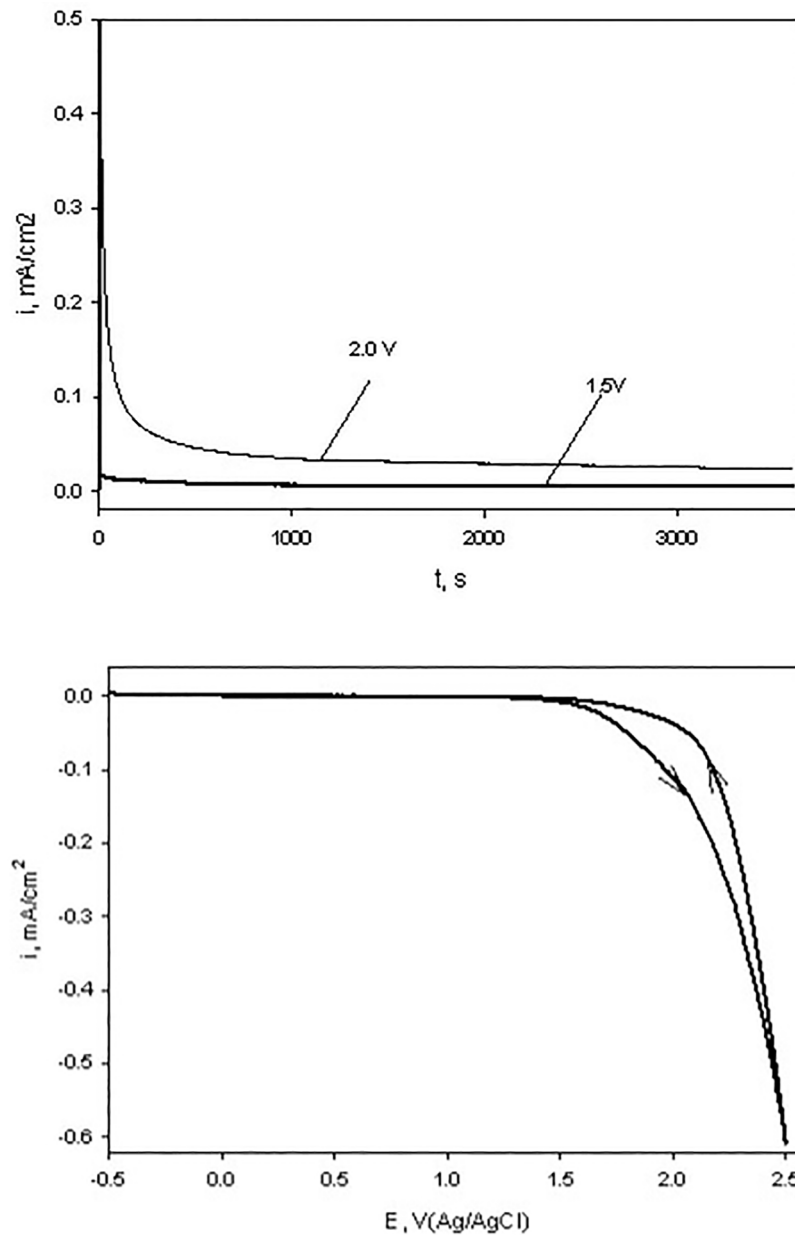
Fig 3. Chronoamperometry curves of the BDD electrode for two fixed potentials (upper panel) and a cyclic voltammetry trace (scan rate v = 10 mV/s, lower panel) in 0.01 mol/L potassium phosphate buffer (pH = 7) + 250 μg/mL DNA.

https://doi.org/10.1371/journal.pone.0190907.g003

Electrogenerated $\cdot OH$ radicals may react with each other forming hydrogen peroxide (H_2O_2), which can either diffuse into the bulk of the electrolyte or oxidize to oxygen (O_2)[48]:

$$2 \cdot OH \rightarrow H_2O_2, \tag{2}$$

$$H_2O_2 \rightarrow O_2 + 2H^+ + e^- \tag{3}$$

The electrochemically-treated DNA was collected immediately following 1 h exposures and processed for GC/MS/MS analysis. Figs 4–8 present the measured concentrations of selected
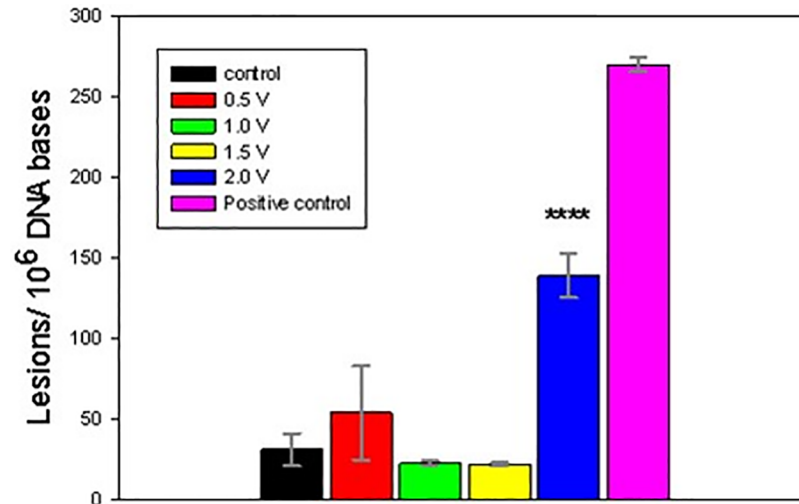
Fig 4. Level of 8-OH-Gua lesions, measured following 1 h DNA electrolysis at four fixed potentials. Asterisks indicate significantly increased lesion level results compared to the control samples using one-way Analysis of Variance (ANOVA) followed by Dunnett's multiple comparison test. The analytical positive control sample was not included in the ANOVA analysis. Four asterisks indicate $p < 0.0001$. Control and fixed potential sample data represent the mean of 5 independent measurements. The analytical positive control data represents the mean of 2 independent measurements. Uncertainties are standard deviations.

lesions produced during incubations at 4 fixed WE potential values plotted alongside the negative (DNA solution kept in the cell at the open circuit) and positive (ct-DNA treated with 40 Gy γ radiation) controls separately. Error bars correspond to one standard deviation calculated for three replicate experiments.
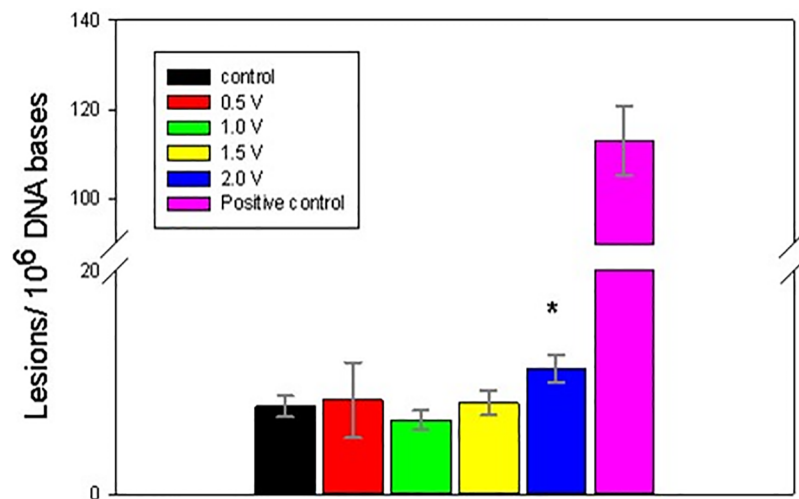
Fig 5. Level of FapyGua lesions, measured following 1 h DNA electrolysis at four fixed potentials. Asterisks indicate significantly increased lesion level results compared to the control samples using one-way Analysis of Variance (ANOVA) followed by Dunnett's multiple comparison test. The analytical positive control sample was not included in the ANOVA analysis. One asterisk indicates $p < 0.05$. Control and fixed potential sample data represent the mean of 5 independent measurements. The analytical positive control data represents the mean of 2 independent measurements. Uncertainties are standard deviations.
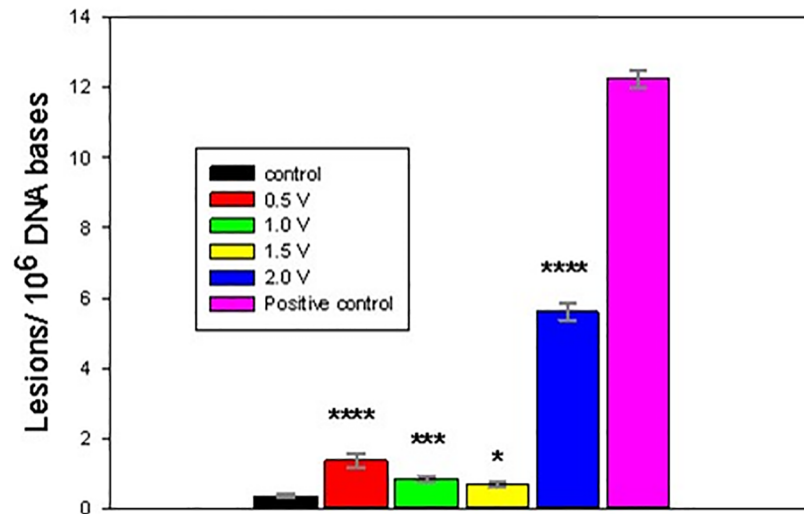
Fig 6. Level of 8-OH-Ade lesions, measured following 1 h DNA electrolysis at four fixed potentials. Asterisks indicate significantly increased lesion level results compared to the control samples using one-way Analysis of Variance (ANOVA) followed by Dunnett's multiple comparison test. The analytical positive control sample was not included in the ANOVA analysis. One, three or four asterisks indicate $p < 0.05$, $p < 0.001$ or $p < 0.0001$, respectively. Control and fixed potential sample data represent the mean of 4 to 5 independent measurements. The analytical positive control data represents the mean of 2 independent measurements. Uncertainties are standard deviations.

https://doi.org/10.1371/journal.pone.0190907.g006

Discussion

Purine lessions

Two potential ranges could be distinguished in the oxidative lesion amount vs electrolysis potential plots: from 0.5V to 1.5V and 2V. The lower potential range includes one electron

Fig 7. Level of FapyAde lesions, measured following 1 h DNA electrolysis at four fixed potentials. Asterisks indicate significantly increased lesion level results compared to the control samples using one-way Analysis of Variance (ANOVA) followed by Dunnett's multiple comparison test. The analytical positive control sample was not included in the ANOVA analysis. One or four asterisks indicate $p < 0.05$ or $p < 0.0001$, respectively. Control and fixed potential sample data represent the mean of 3 to 5 independent measurements. The analytical positive control data represents the mean of 2 independent measurements. Uncertainties are standard deations.
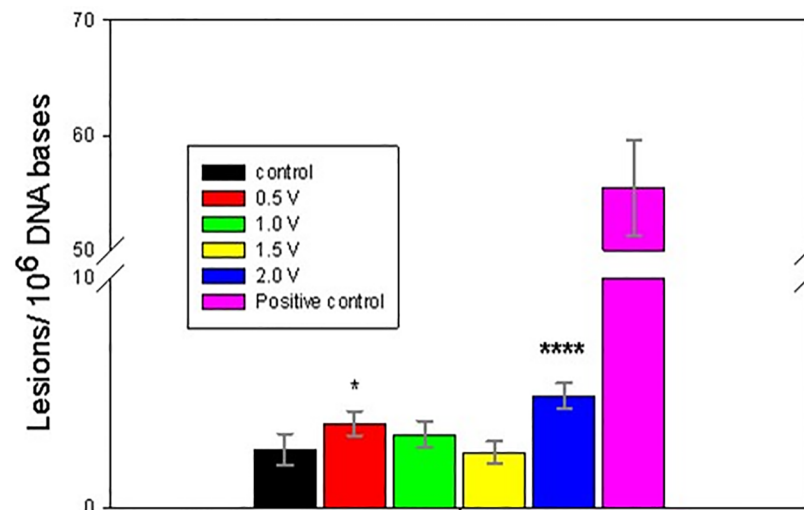
https://doi.org/10.1371/journal.pone.0190907.g007
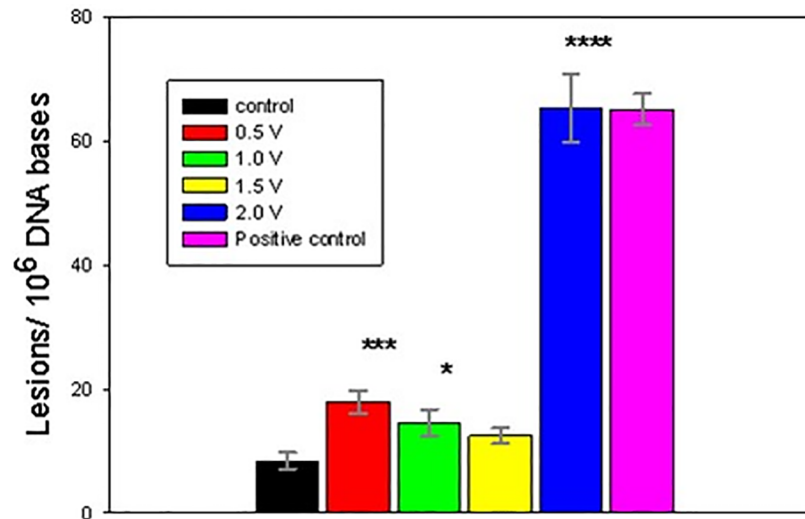
Fig 8. Level of 5-OH-5-MeHyd lesions, measured following 1 h DNA electrolysis at four fixed potentials. Asterisks indicate significantly increased lesion level results compared to the control samples using one-way Analysis of Variance (ANOVA) followed by Dunnett's multiple comparison test. The analytical positive control sample was not included in the ANOVA analysis. One, three or four asterisks indicate $p < 0.05$, $p < 0.001$ or $p < 0.0001$, respectively. Control and fixed potential sample data represent the mean of 4 to 5 independent measurements. The analytical positive control data represents the mean of 2 independent measurements. Uncertainties are standard deviations.

https://doi.org/10.1371/journal.pone.0190907.g008

redox potentials of free purines (E_7 G = 1.1 V, E_7 A = 1.2 V) [15, 17, 27], while E = 2 V exceeds pyrimidine oxidation potentials (E_7 T = 1.7V, E_7 C = 1.6 V) [11, 29] and in addition oxidizing species, such as hydroxyl radicals, hydrogen peroxide and oxygen, which are produced by the BDD WE [38]. As evident from Figs 4–8, after electrolysis at E = 2 V a significant increase in all five measured lesion levels was observed, which happens past the onset of water electrolysis and hydroxyl radical generation at the BDD WE (Fig 3). Somewhat unexpectedly, we did not register a gradual increase in all measured lesions when DNA was exposed at increasing oxidative bias from E = 0.5 V to E = 1.5 V. Amounts of all four purine lesions were rather close to a negative control levels up to E = 1.5 V (Figs 4–7) with evidence suggesting higher levels at the lowest potential of this range (E = 0.5V). The elevated levels of 8-OH-Gua and 8-OH-Ade at E = 0.5 V could be related to a 0.5 V lower lesion oxidation potential with respect to the corresponding intact free bases (Table A in S1 Text) [18, 50–52]. Furthermore, redox potentials of purines and their oxidation intermediates in DNA are further lowered due to purine-purine stacking in the double helix as reported by Burrows et al. [53] and would favor oxidatively-induced lesion generation when equilibrated at E = 0.5V (Figs 4–7). Once formed, these lesions would be vulnerable to further oxidation at increasing positive bias (when exposed at E = 1 V and E = 1.5 V), leading to the appearance of numerous other products (e.g., diamine, diol, guanidinohydantoin) [54] which were not included in the present study. *In vivo*, 8-OH-Gua and 8-OH-Ade are oxidized by tryptophyl (E = 0.9 V), tyrosyl (E = 0.73 V) and thyil (E = 0.55 V) radicals that are located in the histone proteins, covering DNA [23]. Because of its low redox potential 8-OH-Gua was also suggested to play an oxidation protective role for the DNA by serving as an "electron sink" [55].

The first step in the formation of 8-OH-Gua and 8-OH-Ade involves transient 8-OH-Ade adduct radical cation formation [56]. As described by Steenken et al. [57], these radicals are redox ambivalent and could be either reduced or oxidized, depending on the prevailing redox environment. The oxidative pathway will lead to the formation of 8-OH-Gua and 8-OH-Ade
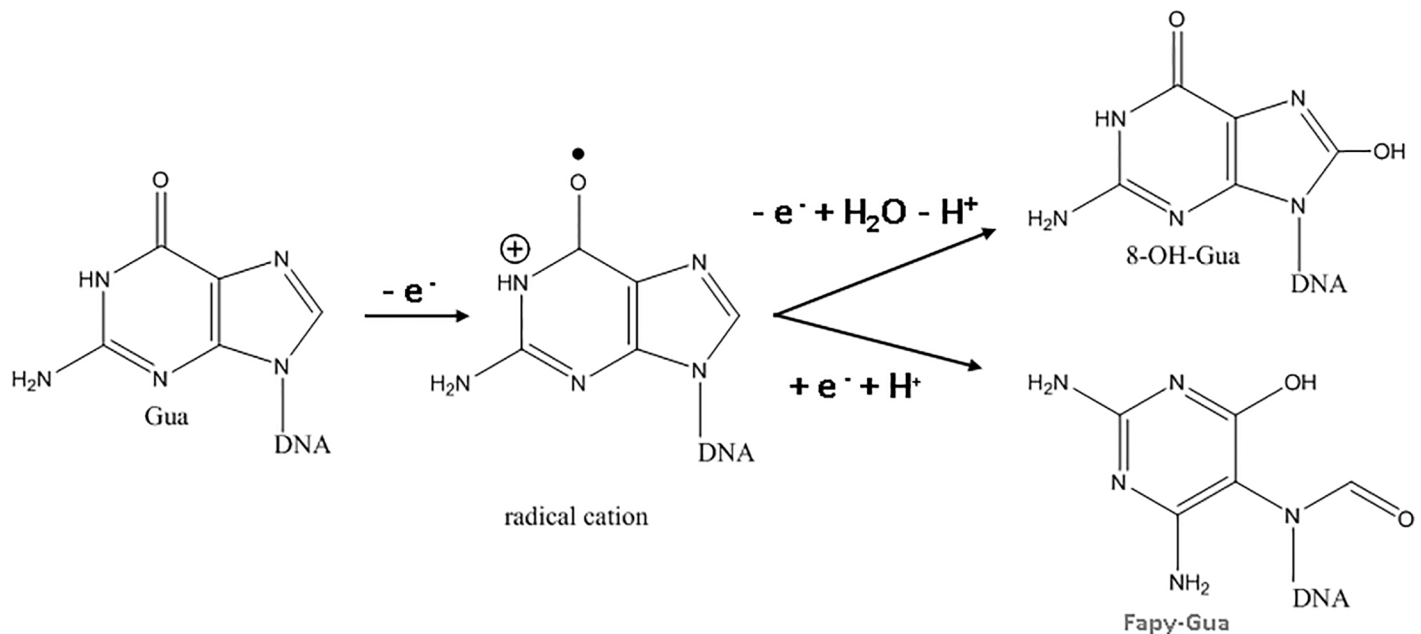
Fig 9. Redox ambivalence of the guanine oxidation intermediate radical cation.

as final products, while the reductive pathway will result in imidazole ring-opened Fapy lesions (Fig 9, Gua only shown, Ade similar).

Both radical cation reaction pathways are consistent with the observed decrease in purine 8-OH and Fapy lesions at higher oxidative (or less reductive) potential in the range from 0.5 V to1.5 V (Figs 4–7). At 0.5 V both 8-OH-Gua and 8-OH-Ade will be exposed close to their redox equilibrium potential and the driving force for further redox conversion will be small resulting in their stabilizations at lower potentials. When the potential is shifted positive, the concentration of the detected lesions will depend on the relative rates of oxidized base formation and their transformation due to subsequent redox and/or chemical reactions. A gradual decrease in the amounts of 8-OH-Gua and 8-OH-Ade lesions from 0.5 V to 1.0 V to 1.5 V may suggest that the intermediate transformation reactions are favored at least up to 2 V, when the •OH radical enabled processes of OH adduct formation and direct H abstraction overcome direct electron abstraction reactions (Figs 4–7). However, bearing in mind the experimental uncertainties, an extended DNA exposure at 0.5 V < E < 1.5 V will be required to underpin the above interpretation.

The 8-OH/Fapy lesion concentration ratio was proposed as a proxy for characterizing the *in vitro* and *in vivo* intracellular redox environment [25, 58]. Furthermore, studies by Malins et al. demonstrated that the concentration ratio of at least one ring-opened (cytotoxic) DNA base lesion to at least one hydroxyl adduct (mutagenic) DNA base lesion could be an accurate diagnostic predictor of a cancerous or non-cancerous specimen [47,48]. It is notable that in our experiments 8-OH-Gua yields were up to ten times higher than FapyGua, however the ratio was reversed for adenine lesions (Table 1). Also, both ratios approached the values in the untreated DNA sample (which was used as a negative control) and to the 40 Gy γ—irradiated positive control except for the sample oxidized at 2 V. DNA treatment at 2 V significantly enhances 8-OH lesion production over their Fapy counterparts (Table 1). Apparently, the continuous presence of the strong oxidizing environment at this potential stabilizes OH adduct

Table 1. DNA lesion concentration ratios for ct-DNA following 1 h electrochemical oxidation at four fixed potentials and 40 Gy γ—irradiation. Values are mean and one standard deviation (n = 3) on three replicates.

Lesion ratio	Negative control, open circuit	E = 0.5V	E = 1.0V	E = 1.5V	E = 2.0V
8-OH-Gua/8-OH-Ade	12.2 +-2.6	14.6+-4.9	7.1+-1.3	9.1+-2.1	28.5+-2.3
FapyGua/FapyAde	21.8+-3.9	6.2+-1.8	7.8+-1.1	12.2+-3.8	2.0+-0.3
8-OH-Gua/FapyGua	4.0+-1.2	6.4+-2.4	3.4+-1.3	2.7+-1.2	12.4+-1.7
8-OH-Ade/FapyAde	0.1+-0.03	0.4+-0.09	0.3+-1.3	0.3+-0.03	1.2+-0.3
8-OH-Gua/5-OH-5-MeHyd	3.7+-0.5	3.0+-0.7	1.6+-0.5	1.6+-0.5	2.1+-0.5

https://doi.org/10.1371/journal.pone.0190907.t001

lesions at the expense of ring-opened ones. Moreover, this stable and high oxidative bias boosts 8-OH-Gua yield, which is almost 30 times higher than 8-OH-Ade at 2 V. While $^{\bullet}$OH radical production is likely the primary reagent in both situations, the redox environments for the bases could differ substantially. Ionizing radiation produces hydrogen atoms and hydrated electrons in addition to $^{\bullet}$OH radicals, which may lower the overall redox potential, as experienced by DNA [54]. High yields of pyrimidine lesions (5-OH-5MeHyd), detected in our DNA samples exposed to 2 V (Fig 8) also suggests the role of strong oxidative bias facilitating the oxidation of OH-adduct radicals of T. Alternatively, due to its lower oxidation potential, electrons from intermediate G radicals can be transferred to A residues in close proximity thus protecting A at the expense of G [59].

Pyrimidine lesions

The initial step in pyrimidine oxidation by direct electron transfer reactions includes efficient formation of radical cations [54, 60] that afterwards transform to stable products through hydration and deprotonation. Hydration leads to OH substituted radicals that are similar in activity to $^{\bullet}$OH radicals [60, 61] while deprotonation leads to uracil. Considering that for pyrimidine bases the redox potentials are higher than for purine (E_7Cyt = 1.6 V, E_7Thy = 1.7 V) [47, 62] direct electron transfer related Thy lesion formation at 2 V would be expected to be slower on thermodynamic basis. It is also possible that pyrimidine radicals react with surrounding purines in a double stranded DNA, and produce tandem lesions [54, 63].

One electron oxidation reaction of Thy produces radical cations that decomposes primarily via hydration reaction, leading to formation of 5-OH-5MeHyd after the addition of oxygen and reduction [64]. It is notable that the Thy lesion level in DNA was significantly higher compared to the Ade lesion levels despite its higher redox potential (Figs 6–8). Similar effects were reported when DNA was oxidized by photosensitization with menadione [65]. A preferential Thy reactivity was related by Joseph et al. to a proton coupled inter-strand electron transfer from the oxidized Thy to Ade due to reactive intermediates in Ade/Thy rich DNA sections [27].

Relationship to the ionizing radiation induced DNA damage. Two main mechanisms are responsible for the formation of radiation induced DNA damage in aqueous environments: first—direct DNA base ionization or electron abstraction due to high energy photon absorption and second—formation of ROS (e.g., $^{\bullet}$OH radicals) via radiolysis of water, which subsequently can attack DNA as previously described [63]. Both mechanisms, however, may lead to similar types of stable purine and pyrimidine decomposition products. In the case of direct electron abstraction, a cation radical is produced which then could undergo deprotonation or hydration. Interaction with the $^{\bullet}$OH radical due to water radiolysis results in either nucleobase OH adduct formation or H atom loss, both pathways creating intermediate radicals [54]. A similar model is conceivable within an electrochemical system: direct electron abstraction

from nucleotides exposed to the electrodes and reactions with ROS, generated at the BDD electrode due to water electrolysis (Eqs (1)–(3) above).

In this context it is instructive to relate electrochemically formed lesions following DNA exposure at increasing oxidation potential with DNA damage products resulting from its exposure to photons with energies close to the DNA base ionization threshold [66, 67]. Equilibration of the DNA with a BDD electrode at a potential exceeding specific nucleobase oxidation potential facilitates one electron oxidation and is analogous to its exposure to the radiation with a photon energy exceeding base electron affinity. A sub-ionization energy photons causes direct electron excitation from HUMO and leads to cyclobutene pyrimidine dimer formation [67]. Therefore, base electron abstraction by the WE mechanistically is comparable to a direct ionization via excitation across the HUMO-LUMO (lowest unoccupied molecular orbital) gap as indicated by the UV light absorbance around 260 nm (also known as X band) [68]. Fig 10 displays nucleobase and base-pair highest occupied molecular orbital (HOMO) energy levels estimated in [69–71] relative to vacuum electron energy (right axis) and on a Ag/AgCl potential scale (left axis). Given the assumptions, used in these calculations, as well as covalent and non-covalent interactions in a double helix, these values are to be treated as approximate, nevertheless the relative nucleic acid base oxidation potentials were experimentally confirmed [14, 20, 32]. As the BDD electrode potential increases, its Fermi level E_f (located at the top of the filled electron energy band for a semi-metal BDD) moves down on an absolute energy scale and allows for a direct charge injection from the HOMO's of nucleobases upon crossing it similar to ionization by a photon when its energy exceeds nucleobase electron affinity. The efficient charge transport through DNA would facilitate redox equilibration with nucleotides that may not be in direct contact with the electrode surface [72, 73].

In the present work, the goal was to quantify the extent of DNA damage induced by exhaustive electro-oxidation under well controlled conditions that mimic the effects of oxidative stress, caused by oxygen metabolism, chemical toxicants and ionizing radiation. We have shown that equilibrating soluble nucleic acids with a high surface area BDD WE maintained at a constant potential leads to oxidatively induced DNA damage. Five DNA lesions were
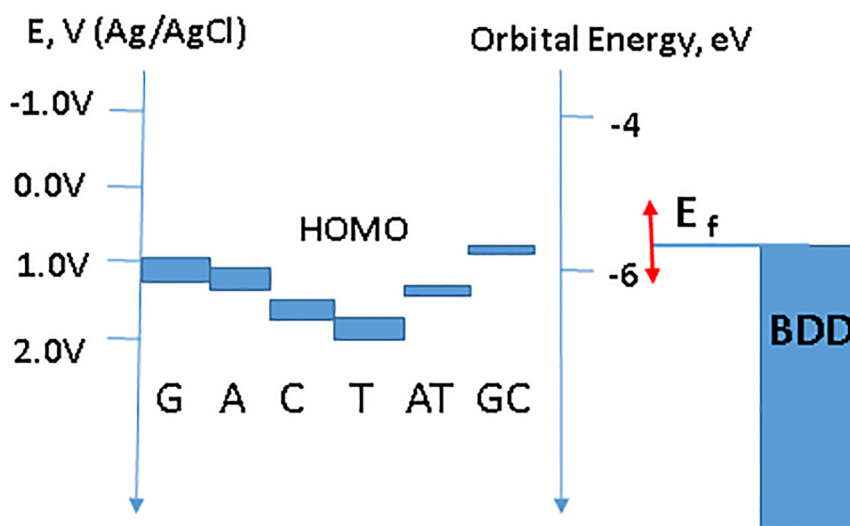
Fig 10. Schematic representation of the nucleic acid base highest occupied molecular orbital (HOMO) in aqueous solutions relative to the electrochemical potential scale. HOMO values are from [65–68] with bar widths representing a spread in literature values. BDD shows a continuum of the anode electronic density, red arrow—Fermi level variation with applied potential (see text).

https://doi.org/10.1371/journal.pone.0190907.g010

identified and measured by GC/MS/MS: FapyAde, FapyGua, 8-OH-Gua, 5-OH-5-MeHyd and 8-OH-Ade. There were two base lesion formation modes detected in the explored electrode potential range, corresponding to 0.5 V < E < 1.5 V and E > 1.5 V. Amounts of all four purine lesions were rather close to a negative control levels up to E = 1.5 V (Figs 4–7) with evidence suggesting higher levels at the lowest potential of this range (E = 0.5 V). A statistically significant gradual drop in some measured lesions (8-OH-Ade; FapyAde, and 5-OH-5-MeHyd; Figs 6–8) was detected when DNA was exposed at increasingly higher fixed BDD WE potentials from E = 0.5 V to E = 1.5 V. We hypothesize that it could be related to the lower redox potentials of the base OH adduct lesions and redox ambivalence of the base radical cations. A substantial rise in all base lesion yields was measured when DNA was exposed at E = 2 V, when $^{\bullet}$OH radicals are known to be efficiently produced by the BDD electrode. We recorded an almost 30 times higher 8-OH-Gua yield than 8-OH-Ade at E = 2 V, which also surpasses a similar ratio for a 40 Gy γ -irradiated sample. Taken together with the evidence of the elevated yields of pyrimidine lesions at this potential it shows that a stable redox bias in an electrochemical cell facilitates further base OH-adduct radical oxidation.

Conclusions

Exhaustive DNA electrooxidation at tightly controlled potentiostatic conditions allows for the selective generation of oxidatively modified DNA lesions by either direct electron transfer or by $^{\bullet}$OH radical reactions. A 1 h exposure of solution-state ct-DNA to a BDD WE, biased from 0.5 V to 2 V (vs Ag/AgCl) offers a viable method for generating an oxidative environment without the need for chemical oxidants. This experimental approach may be helpful for the development of DNA damage reference materials, a critical measurement element in establishing a quantitative link between DNA degradation and disease.

NIST Disclaimer

Certain commercial equipment, instruments and materials are identified in this paper to specify an experimental procedure as completely as possible. In no case does the identification of particular equipment or materials imply a recommendation or endorsement by the National Institute of Standards and Technology nor does it imply that the materials, instruments, or equipment are necessarily the best available for the purpose.

Supporting information

S1 Text. Detailed methodology for GC/MS/MS determination of DNA base lesion profiles. (DOCX)

Author Contributions

Conceptualization: Vytas Reipa, Bryant C. Nelson.

Data curation: Donald H. Atha, Sanem H. Coskun, Christopher M. Sims.

Formal analysis: Bryant C. Nelson.

Investigation: Vytas Reipa, Donald H. Atha.

Methodology: Vytas Reipa.

References

1. Dizdaroglu M. Introduction to serial reviews on oxidative DNA damage and repair. Free Radical Bio Med. 2002; 32(8):677- https://doi.org/10.1016/S0891-5849(02)00766-9

2. Cadet J, Delatour T, Douki T, Gasparutto D, Pouget JP, Ravanat JL, et al. Hydroxyl radicals and DNA base damage. Mutat Res-Fund Mol M. 1999; 424(1–2):9–21. https://doi.org/10.1016/S0027-5107(99)00004-4

3. Moller P, Cooke MS, Collins A, Olinski R, Rozalski R, Loft S. Harmonising measurements of 8-oxo-7,8-dihydro-2′-deoxyguanosine in cellular DNA and urine. Free radical research. 2012; 46(4):541–53. https://doi.org/10.3109/10715762.2011.644241 PMID: 22117555

4. Collins AR, Brown J, Bogdanov M, Cadet J, Cooke M, Douki T, et al. Comparison of different methods of measuring 8-oxoguanine as a marker of oxidative DNA damage. Free radical research. 2000; 32 (4):333–41. https://doi.org/10.1080/10715760000300331 PMID: 10741854

5. Sies H. Strategies of Antioxidant Defense. European Journal of Biochemistry. 1993; 215(2):213–9. https://doi.org/10.1111/j.1432-1033.1993.tb18025.x PMID: 7688300

6. Wardman P. Reduction Potentials of One-Electron Couples Involving Free-Radicals in Aqueous-Solution. J Phys Chem Ref Data. 1989; 18(4):1637–755.

7. Rao PS, Hayon E. Redox Potentials of Free-Radicals .4. Superoxide and Hydroperoxy Radicals Single Bond O2- and Single Bond Ho2. J Phys Chem-Us. 1975; 79(4):397–402. https://doi.org/10.1021/j100571a021

8. Ivanova AV, Gerasimova EL, Brainina KZ. Potentiometric Study of Antioxidant Activity: Development and Prospects. Crit Rev Anal Chem. 2015; 45(4):311–22. https://doi.org/10.1080/10408347.2014.910443 PMID: 25830410

9. Halliwell B. Biochemistry of oxidative stress. Biochem Soc T. 2007; 35:1147–50.

10. Brett CMA, Brett AMO, Serrano SHP. On the Adsorption and Electrochemical Oxidation of DNA at Glassy-Carbon Electrodes. J Electroanal Chem. 1994; 366(1–2):225–31. https://doi.org/10.1016/0022-0728(93)02994-S

11. Faraggi M, Broitman F, Trent JB, Klapper MH. One-electron oxidation reactions of some purine and pyrimidine bases in aqueous solutions. Electrochemical and pulse radiolysis studies. J Phys Chem-Us. 1996; 100(35):14751–61. https://doi.org/10.1021/jp960590g

12. Palecek E, Bartosik M. Electrochemistry of Nucleic Acids. Chem Rev. 2012; 112(6):3427–81. https://doi.org/10.1021/cr200303p PMID: 22372839

13. Cahova-Kucharikova K, Fojta M, Mozga T, Palecek E. Use of DNA repair enzymes in electrochemical detection of damage to DNA bases in vitro and in cells. Anal Chem. 2005; 77(9):2920–7. https://doi.org/10.1021/ac048423x PMID: 15859612

14. Boussicault F, Robert M. Electron transfer in DNA and in DNA-related biological processes. Electrochemical insights. Chem Rev. 2008; 108(7):2622–45. https://doi.org/10.1021/cr0680787 PMID: 18563937

15. Akhavan O, Ghaderi E, Rahighi R. Toward Single-DNA Electrochemical Biosensing by Graphene Nanowalls. Acs Nano. 2012; 6(4):2904–16. https://doi.org/10.1021/nn300261t PMID: 22385391

16. Goyal RN, Sangal A. Insights into the oxidation chemistry of 2-hydroxypurine by electrochemical methods. Electroanal. 2005; 17(3):246–54. https://doi.org/10.1002/elan.200303087

17. Goyal RN, Sondhi SM, Lahoti AM. Investigations of electron-transfer reactions and the redox mechanism of 2′-deoxyguanosine-5′-monophosphate using electrochemical techniques. New J Chem. 2005; 29(4):587–95. https://doi.org/10.1039/b415452p

18. Goyal RN, Dhawan A. Insights into the biological redox chemistry of 2′-deoxyadenosine 5′-monophosphate by electrochemical techniques. B Chem Soc Jpn. 2005; 78(11):1944–52. https://doi.org/10.1246/bcsj.78.1944

19. Nowicka AM, Zabost E, Gilant E, Stojek Z. Influence of percentage of guanine molecules, OH radicals, UV irradiation and temperature on electrooxidation of short synthetic oligonucleotides. Phys Chem Chem Phys. 2011; 13(16):7500–7. https://doi.org/10.1039/c0cp02667k PMID: 21423983

20. Oliveira-Brett AM, Piedade JAP, Silva LA, Diculescu VC. Voltammetric determination of all DNA nucleotides. Analytical biochemistry. 2004; 332(2):321–9. https://doi.org/10.1016/j.ab.2004.06.021 PMID: 15325301

21. Johnston DH, Campbell K, Thorp HH. Electron-Transfer Reactions between DNA and Metal-Complexes—Model Studies for Ionizing-Radiation Damage. Abstr Pap Am Chem S. 1995; 209:543-Inor.

22. Boal AK, Barton JK. Electrochemical detection of lesions in DNA. Bioconjugate Chem. 2005; 16 (2):312–21. https://doi.org/10.1021/bc0497362 PMID: 15769084

23. Steenken S, Jovanovic SV. How easily oxidizable is DNA? One-electron reduction potentials of adenosine and guanosine radicals in aqueous solution. J Am Chem Soc. 1997; 119(3):617–8. https://doi.org/10.1021/ja962255b

24. Cadet J, Carell T, Cellai L, Chatgilialoglu C, Gimisis T, Miranda M, et al. DNA damage and radical reactions: Mechanistic aspects, formation in cells and repair studies. Chimia. 2008; 62(9):742–9. https://doi.org/10.2533/chimia.2008.742

25. Malins DC. Identification of Hydroxyl Radical-Induced Lesions in DNA-Base Structure—Biomarkers with a Putative Link to Cancer Development. J Toxicol Env Health. 1993; 40(2–3):247–61.

26. Cadet J, Wagner JR. DNA Base Damage by Reactive Oxygen Species, Oxidizing Agents, and UV Radiation. Csh Perspect Biol. 2013; 5(2). https://doi.org/10.1101/cshperspect.a012559 PMID: 23378590

27. Joseph J, Schuster GB. One-electron oxidation of DNA: reaction at thymine. Chem Commun. 2010; 46 (42):7872–8. https://doi.org/10.1039/c0cc02118k PMID: 20830420

28. Gasparutto D, Ait-Abbas M, Jaquinod M, Boiteux S, Cadet J. Repair and coding properties of 5-hydroxy-5-methylhydantoin nucleosides inserted into DNA oligomers. Chem Res Toxicol. 2000; 13 (7):575–84. https://doi.org/10.1021/tx000005+ PMID: 10898589

29. Ivandini TA, Honda K, Rao TN, Fujishima A, Einaga Y. Simultaneous detection of purine and pyrimidine at highly boron-doped diamond electrodes by using liquid chromatography. Talanta. 2007; 71(2):648–55. https://doi.org/10.1016/j.talanta.2006.05.009 PMID: 19071355

30. Kubar T, Gutierrez R, Kleinekathofer U, Cuniberti G, Elstner M. Modeling charge transport in DNA using multi-scale methods. Phys Status Solidi B. 2013; 250(11):2277–87. https://doi.org/10.1002/pssb.201349148

31. Boon EM, Barton JK. DNA Electrochemistry as a probe of base pair stacking in A-, B-, and Z-form DNA. Bioconjugate Chem. 2003; 14(6):1140–7. https://doi.org/10.1021/bc034139l PMID: 14624627

32. Hawke LGD, Kalosakas G, Simserides C. Electronic parameters for charge transfer along DNA. Eur Phys J E. 2010; 32(3):291–305. https://doi.org/10.1140/epje/i2010-10650-y PMID: 20680380

33. Goyal RN, Dhawan A. Oxidation chemistry of 2′-deoxyadenosine at pyrolytic graphite electrode. Bioelectrochemistry. 2006; 69(2):223–33. https://doi.org/10.1016/j.bioelechem.2006.03.003 PMID: 16675309

34. Goyal RN, Tyagi A. Investigations into the electrooxidation of guanosine-5′-triphosphate at the pyrolytic graphite electrode. Anal Bioanal Chem. 2005; 382(7):1683–90. https://doi.org/10.1007/s00216-005-3344-8 PMID: 16007444

35. Baumann A, Lohmann W, Jahn S, Karst U. On-Line Electrochemistry/Electrospray Ionization Mass Spectrometry (EC/ESI-MS) for the Generation and Identification of Nucleotide Oxidation Products. Electroanal. 2010; 22(3):286–92. https://doi.org/10.1002/elan.200900358

36. Atha DH, Ammanamanchi N, Obadina M, Reipa V. Quantitative Measurement of Electrochemically Induced DNA Damage Using Capillary Electrophoresis. J Electrochem Soc. 2013; 160(7):G3139–G43. https://doi.org/10.1149/2.021307jes

37. Martinez-Huitle CA, Rodrigo MA, Sires I, Scialdone O. Single and Coupled Electrochemical Processes and Reactors for the Abatement of Organic Water Pollutants: A Critical Review. Chem Rev. 2015; 115 (24):13362–407. https://doi.org/10.1021/acs.chemrev.5b00361 PMID: 26654466

38. Comninellis C, Kapalka A, Malato S, Parsons SA, Poulios L, Mantzavinos D. Advanced oxidation processes for water treatment: advances and trends for R&D. J Chem Technol Biot. 2008; 83(6):769–76. https://doi.org/10.1002/jctb.1873

39. Kapalka A, Foti G, Comninellis C. The importance of electrode material in environmental electrochemistry Formation and reactivity of free hydroxyl radicals on boron-doped diamond electrodes. Electrochim Acta. 2009; 54(7):2018–23. https://doi.org/10.1016/j.electacta.2008.06.045

40. Porsch B, Laga R, Horsky J, Konak C, Ulbrich K. Molecular Weight and Polydispersity of Calf-Thymus DNA: Static Light-Scattering and Size-Exclusion Chromatography with Dual Detection. Biomacromolecules. 2009; 10(11):3148–50. https://doi.org/10.1021/bm900768j PMID: 19817429

41. Petersen EJ, Tu XM, Dizdaroglu M, Zheng M, Nelson BC. Protective Roles of Single-Wall Carbon Nanotubes in Ultrasonication-Induced DNA Base Damage. Small. 2013; 9(2):205–8. https://doi.org/10.1002/smll.201201217 PMID: 22987483

42. Hunt PR, Marquis BJ, Tyner KM, Conklin S, Olejnik N, Nelson BC, et al. Nanosilver suppresses growth and induces oxidative damage to DNA in Caenorhabditis elegans. J Appl Toxicol. 2013; 33(10):1131–42. Epub 2013/05/03. https://doi.org/10.1002/jat.2872 PMID: 23636779.

43. Hunt PR. The C. elegans model in toxicity testing. Journal of applied toxicology: JAT. 2017; 37(1):50–9. https://doi.org/10.1002/jat.3357 PMID: 27443595.

44. Reddy PT, Jaruga P, Kirkali G, Tuna G, Nelson BC, Dizdaroglu M. Identification and quantification of human DNA repair protein NEIL1 by liquid chromatography/isotope-dilution tandem mass spectrometry. J Proteome Res. 2013; 12(2):1049–61. Epub 2012/12/28. https://doi.org/10.1021/pr301037t PMID: 23268652.

45. Reddy PT, Jaruga P, Kirkali G, Tuna G, Nelson BC, Dizdaroglu M. Identification and Quantification of Human DNA Repair Protein NEIL1 by Liquid Chromatography/Isotope-Dilution Tandem Mass Spectrometry. Journal of proteome research. 2013; 12(2):1049–61. https://doi.org/10.1021/pr301037t PMID: 23268652

46. Jaruga P, Coskun E, Kimbrough K, Jacob A, Johnson WE, Dizdaroglu M. Biomarkers of oxidatively induced DNA damage in dreissenid mussels: A genotoxicity assessment tool for the Laurentian Great Lakes. Environ Toxicol. 2017. https://doi.org/10.1002/tox.22427 PMID: 28568507.

47. Brotons A, Vidal-Iglesias FJ, Solla-Gullon J, Iniesta J. Carbon materials for the electrooxidation of nucleobases, nucleosides and nucleotides toward cytosine methylation detection: a review. Anal Methods-Uk. 2016; 8(4):702–15. https://doi.org/10.1039/c5ay02616d

48. Michaud PA, Panizza M, Ouattara L, Diaco T, Foti G, Comninellis C. Electrochemical oxidation of water on synthetic boron-doped diamond thin film anodes. J Appl Electrochem. 2003; 33(2):151–4. https://doi.org/10.1023/A:1024084924058

49. Marselli B, Garcia-Gomez J, Michaud PA, Rodrigo MA, Comninellis C. Electrogeneration of hydroxyl radicals on boron-doped diamond electrodes. J Electrochem Soc. 2003; 150(3):D79–D83. https://doi.org/10.1149/1.1553790

50. Gupta P, Oyama M, Goyal RN. Electrochemical investigations of 8-hydroxydeoxyguanosine and its determination at an edge plane pyrolytic graphite electrode. Rsc Adv. 2016; 6(3):1722–8. https://doi.org/10.1039/c5ra22682a

51. Steenken S, Jovanovic SV, Bietti M, Bernhard K. The trap depth (in DNA) of 8-oxo-7,8-dihydro-2´ deoxyguanosine as derived from electron-transfer equilibria in aqueous solution. J Am Chem Soc. 2000; 122 (10):2373–4. https://doi.org/10.1021/ja993508e

52. Goyal RN, Jain N, Garg DK. Electrochemical and enzymic oxidation of guanosine and 8-hydroxyguanosine and the effects of oxidation products in mice. Bioelectroch Bioener. 1997; 43(1):105–14. https://doi.org/10.1016/S0302-4598(96)05182-3

53. Burrows CJ, Muller JG. Oxidative nucleobase modifications leading to strand scission. Chem Rev. 1998; 98(3):1109–51. https://doi.org/10.1021/cr960421s PMID: 11848927

54. Dizdaroglu M, Jaruga P, Birincioglu M, Rodriguez H. Free radical-induced damage to DNA: Mechanisms and measurement. Free Radical Bio Med. 2002; 32(11):1102–15. https://doi.org/10.1016/S0891-5849(02)00826-2

55. Kanvah S, Schuster GB. The sacrificial role of easily oxidizable sites in the protection of DNA from damage. Nucleic acids research. 2005; 33(16):5133–8. https://doi.org/10.1093/nar/gki801 PMID: 16157862

56. Cadet J, Bardet M, Berger M, Berthod T, Delatour T, D'Ham C, et al. Oxidative base damage to DNA—Recent mechanistic aspects, measurement and repair. Nato Adv Sci I a-Lif. 1999; 302:47–58.

57. Steenken S. Purine-Bases, Nucleosides, and Nucleotides—Aqueous-Solution Redox Chemistry and Transformation Reactions of Their Radical Cations and E- and Oh Adducts. Chem Rev. 1989; 89 (3):503–20. https://doi.org/10.1021/cr00093a003

58. Malins DC, Haimanot R. Major Alterations in the Nucleotide Structure of DNA in Cancer of the Female Breast. Cancer research. 1991; 51(19):5430–2. PMID: 1655250

59. Bergeron F, Auvre F, Radicella JP, Ravanat JL. HO center dot radicals induce an unexpected high proportion of tandem base lesions refractory to repair by DNA glycosylases. Proceedings of the National Academy of Sciences of the United States of America. 2010; 107(12):5528–33. https://doi.org/10.1073/pnas.1000193107 PMID: 20212167

60. Wagner JR, Cadet J. Oxidation Reactions of Cytosine DNA Components by Hydroxyl Radical and One-Electron Oxidants in Aerated Aqueous Solutions. Accounts Chem Res. 2010; 43(4):564–71. https://doi.org/10.1021/ar9002637 PMID: 20078112

61. Wagner JR, Hu CC, Ames BN. Endogenous Oxidative Damage of Deoxycytidine in DNA. Proceedings of the National Academy of Sciences of the United States of America. 1992; 89(8):3380–4. https://doi.org/10.1073/pnas.89.8.3380 PMID: 1565630

62. Thapa B, Schlegel HB. Calculations of pK(a)'s and Redox Potentials of Nucleobases with Explicit Waters and Polarizable Continuum Solvation. J Phys Chem A. 2015; 119(21):5134–44. https://doi.org/10.1021/jp5088866 PMID: 25291241

63. Ravanat JL, Douki T. UV and ionizing radiations induced DNA damage, differences and similarities. Radiat Phys Chem. 2016; 128:92–102. https://doi.org/10.1016/j.radphyschem.2016.07.007

64. Cadet J, Wagner JR, Shafirovich V, Geacintov NE. One-electron oxidation reactions of purine and pyrimidine bases in cellular DNA. Int J Radiat Biol. 2014; 90(6):423–32. https://doi.org/10.3109/09553002.2013.877176 PMID: 24369822

65. Bergeron F, Houde D, Hunting DJ, Wagner JR. Electron transfer in DNA duplexes containing 2-methyl-1,4-naphthoquinone. Nucleic acids research. 2004; 32(21):6154–63. https://doi.org/10.1093/nar/gkh950 PMID: 15585661

66. Crespo-Hernandez CE, Arce R, Ishikawa Y, Gorb L, Leszczynski J, Close DM. Ab initio ionization energy thresholds of DNA and RNA bases in gas phase and in aqueous solution. J Phys Chem A. 2004; 108(30):6373–7. https://doi.org/10.1021/jp049270k

67. Kielbassa C, Roza L, Epe B. Wavelength dependence of oxidative DNA damage induced by UV and visible light. Carcinogenesis. 1997; 18(4):811–6. https://doi.org/10.1093/carcin/18.4.811 PMID: 9111219

68. Voet D, Gratzer WB, Cox RA, Doty P. Absorption Spectra of Nucleotides, Polynucleotides, and Nucleic Acids in the Far Ultraviolet. Biopolymers. 1963; 1(3):193–208. https://doi.org/10.1002/bip.360010302

69. Wang LL, Zhang L, Wang H, Zhang Y, Huang JT, Zhu H, et al. Photoinduced Electron Transfer between Anionic Corrole and DNA. J Phys Chem A. 2016; 120(4):535–42. https://doi.org/10.1021/acs.jpca.5b11021 PMID: 26752116

70. Close DM. Calculation of the ionization potentials of the DNA bases in aqueous medium. J Phys Chem A. 2004; 108(46):10376–9. https://doi.org/10.1021/jp046660y

71. Close DM, Wardman P. Calculations of the Energetics of Oxidation of Aqueous Nucleosides and the Effects of Prototropic Equilibria. J Phys Chem A. 2016; 120(23):4043–8. https://doi.org/10.1021/acs.jpca.6b02653 PMID: 27219530

72. Grodick MA, Muren NB, Barton JK. DNA Charge Transport within the Cell. Biochemistry. 2015; 54 (4):962–73. https://doi.org/10.1021/bi501520w PMID: 25606780

73. Nunez ME, Holmquist GP, Barton JK. Evidence for DNA charge transport in the nucleus. Biochemistry. 2001; 40(42):12465–71. https://doi.org/10.1021/bi011560t PMID: 11601969